NASA Public Access
Author manuscript
*J Geophys Res Space Phys*. Author manuscript; available in PMC 2020 August 31.

Published in final edited form as:
*J Geophys Res Space Phys*. 2019 April ; 124(4): 3100–3109. doi:10.1029/2018ja026266.

# Mars's Dayside Upper Ionospheric Composition Is Affected by Magnetic Field Conditions

**Paul Withers**[1,2], **C. L. Flynn**[1], **M. F. Vogt**[2], **M. Mayyasi**[2], **P. Mahaffy**[3], **M. Benna**[3], **M. Elrod**[3], **J. P. McFadden**[4], **P. Dunn**[4], **G. Liu**[4], **L. Andersson**[5], **S. England**[6]

[1]Department of Astronomy, Boston University, Boston, MA, USA,

[2]Center for Space Physics, Boston University, Boston, MA, USA,

[3]Planetary Environments Laboratory, NASA Goddard Space Flight Center, Greenbelt, MD, USA,

[4]Space Sciences Laboratory, University of California, Berkeley, CA, USA,

[5]Laboratory for Atmospheric and Space Physics, University of Colorado Boulder, Boulder, CO, USA,

[6]Department of Aerospace and Ocean Engineering, Virginia Tech, Blacksburg, VA, USA

## Abstract

Previous observations have shown that electron density and temperature in the dayside ionosphere of Mars vary between strongly and weakly magnetized regions of the planet. Here we use data from the Neutral Gas and Ion Mass Spectrometer (NGIMS) on the Mars Atmosphere and Volatile EvolutioN (MAVEN) spacecraft to examine whether dayside ion densities and ionospheric composition also vary. We find that $O^+$, $O_2^+$, and $CO_2^+$ densities above ~200 km are greater in strongly magnetized regions than in weakly magnetized regions. Fractional abundances of ion species are also affected. The $O^+/O_2^+$ ratio at 300-km altitude increases from ~0.5 in strongly magnetized regions to ~0.8 in weakly magnetized regions. Consequently, the plasma reservoir available for escape is fundamentally different between strongly magnetized and weakly magnetized regions.

## 1. Introduction

Although lacking a global-scale internally-generated magnetic field, Mars possesses localized areas of strong magnetic field (Acuña et al., 1999; Connerney et al., 1999). These are caused by coherent thermal remanent magnetization in regions of the planet's crust that formed prior to the failure of the presumed internal dynamo and that have not been subsequently disrupted by large impacts (Acuña et al., 2001; Connerney et al., 2001). The

**Correspondence to:** P. Withers, withers@bu.edu.

Supporting Information:
- Supporting Information S1
- Figure S1

NASA Author Manuscript
NASA Author Manuscript
NASA Author Manuscript

NASA Author Manuscript NASA Author Manuscript NASA Author Manuscript

strongest crustal field regions are found at southern latitudes and longitudes of 120°E to 240°E (e.g., Brain et al., 2003; Connerney et al., 2001).

The unusual magnetic environment of Mars, which is noticeably different from the strong, global-scale dipolar magnetization of Earth and from the nonexistent internal magnetization of Venus, affects the planet's surrounding plasma environment. Despite their limited spatial extent, the crustal field regions have substantial effects on the planet's interaction with the solar wind (e.g., Edberg et al., 2008; Mitchell et al., 2001).

Crustal field regions affect the loss of volatiles to space and hence affect the history of the climate of Mars. A comprehensive and well-referenced discussion is provided by Fang et al. (2017). Brecht and Ledvina (2014) applied a hybrid particle code (HALFSHEL) to investigate the interaction of Mars and the solar wind. They found that the presence of crustal magnetic fields reduces the ion loss rate and also modifies the energy spectrum of escaping ions. Observational validation of these simulations was provided by comparison of Mars Express ASPERA IMA data to simulations. Observed and simulated dependence of loss rates on solar activity agreed when crustal fields were included in the simulation, but disagreed when crustal fields were omitted. Dong et al. (2015) coupled three global models of the environment of Mars and applied them to investigate how ion loss rate depends on crustal field orientation. They found that Mars season and crustal field orientation with respect to the Sun both affected simulated loss rates, giving a more complicated picture than earlier work that had suggested that a particular crustal field orientation was invariably associated with minimum ion loss rates. Overall, they concluded that crustal fields shield Mars from solar wind interactions and reduce ion loss rates. Fang et al. (2017) used a 3-D multispecies, single-fluid magnetohydrodynamic model to investigate the effects of crustal field regions on boundaries in the plasma environment of Mars and associated implications for escape rates. They found that seasonal and diurnal variations in the Sun-fixed location of crustal field regions are responsible for over half the variation in total ion loss rates. Furthermore, they suggested that crustal fields have two competing effects on ion loss rates. The first effect of crustal field regions is the elevation of the bow shock and induced magnetospheric boundary/magnetic pileup boundary, which shields the atmosphere and ionosphere from the solar wind and reduces ion loss rates. The second effect of crustal field regions is to enhance dayside-to-nightside trans-terminator flow, which leads to increased ion loss rates. This is broadly similar to analogous behavior at Venus when altitudes of plasma boundaries vary due to variations in solar wind dynamic pressure.

Furthermore, ionospheric conditions themselves are also affected by the presence of strong crustal magnetic fields. In a recent analysis, Flynn et al. (2017) found that Mars Atmosphere and Volatile EvolutioN (MAVEN) Langmuir Probe and Waves (LPW; Andersson et al., 2015; Ergun et al., 2015) observations of dayside ionospheric electron density and temperature depended on magnetic field conditions. Between 200- and 400-km altitudes, Flynn et al. (2017) found that regions of strong crustal magnetic fields have larger electron densities and smaller electron temperatures than regions of weak crustal magnetic field. Similar results for density were previously reported by Andrews, Edberg, et al. (2015) and Andrews, Andersson, et al. (2015). The influence of crustal magnetic fields on the nightside ionosphere has been investigated by Girazian et al. (2017). They found that "nightside ion

NASA Author Manuscript NASA Author Manuscript NASA Author Manuscript

densities are … smaller near strong crustal fields," opposite from the dayside results of Flynn et al. (2017). The nightside trends were interpreted as being caused by the effects of strong crustal fields on suprathermal electron fluxes, which are an important ion source on the nightside. Unless the field direction is radial, strong crustal fields impede the influx of suprathermal electrons into the ionosphere.

Yet Flynn et al. (2017) found that neutral densities and temperatures at these altitudes did not depend on magnetic field conditions. Flynn et al. (2017) hypothesized that the dependence of electron densities and temperatures on magnetic field conditions could be associated with the topology of magnetic field lines. Closed field lines on which electrons can be trapped are more common in regions of strong crustal magnetic fields than regions of weak crustal magnetic fields. If trapped on a closed field line, electrons are shielded from solar wind-driven loss processes. The resultant longer plasma lifetime would lead to higher electron densities as the balance between plasma production and loss adjusts to a new equilibrium. It would also lead to lower electron temperatures as electrons, which generally have elevated temperatures upon their production, have longer to cool down.

Sakai et al. (2016), Sakai et al. (MAVEN observations of electron temperatures in the dayside ionosphere at Mars, AGU Fall Meeting Abstract P13A-1921, 2016), and Fang et al. (Mars crustal magnetic fields and large-scale dayside ionospheric anomaly, AGU Fall Meeting Abstract P51C-2610, 2017) used numerical simulations to investigate the dependence of ionospheric properties on magnetic field conditions. Sakai et al. (2016) explained low electron temperatures in regions of strong crustal magnetic fields as being due to efficient heat conduction. On the whole, the magnetic field is more vertical in regions of strong crustal magnetic fields than in regions of weak crustal fields where the magnetic field is draped due to interactions with the solar wind. Vertical field lines enhance the transport of heat from hot plasma at high altitudes to cooler plasma at low altitudes, where the denser neutral atmosphere enhances other cooling processes that remove heat from the electron population. By contrast, vertical heat conduction is suppressed by horizontal draped magnetic fields prevalent in regions of weak crustal fields.

These results described how the electron component of the dayside ionosphere is affected by magnetic field conditions, but did not address how the ion component of the ionosphere is affected. The simplest possible scenario is that ion composition is insensitive to magnetic field conditions. In this scenario, densities of all ion species change in lock-step with the electron density, which equals the total ion density. But this scenario is unlikely to be applicable: Since electron temperature affects chemical reaction rates and vertical transport rates, the previously observed variations in electron properties with magnetic field conditions are likely to be accompanied by variations in ion composition. Motivated by these considerations, the aim of this paper is to determine how the composition of the dayside ionosphere is affected by crustal magnetic field conditions. We will primarily analyze ion density measurements acquired at southern latitudes by the MAVEN Neutral Gas and Ion Mass Spectrometer (NGIMS; Benna et al., 2015; Mahaffy et al., 2015).

The structure of this article is as follows. Section 2 summarizes the data used. Section 3 presents analysis and results concerning ion densities. Section 4 presents analysis and results

NASA Author Manuscript

NASA Author Manuscript

NASA Author Manuscript

concerning ionospheric composition. Section 5 validates MAVEN NGIMS ion density data against data from the MAVEN SupraThermal and Thermal Ion Composition (STATIC) instrument. Section 6 assesses the effects of magnetic field conditions on MAVEN NGIMS neutral density measurements. Section 7 reports the conclusions of this work.

## 2. Data

We surveyed MAVEN NGIMS data from 1 October 2014 to 31 March 2018, which corresponds to $Ls$ = 206°, Mars Year 32 to $Ls$ = 152°, Mars Year 34. The typical periapsis altitude is ~150 km, although this interval includes several “deep dips” in which periapsis was lowered to ~120–130 km for periods of 1 week. However, we show only data above 200-km altitude as no significant trends with magnetic field conditions were apparent at lower altitudes. We used only data at solar zenith angles less than 90°. These NGIMS data cover a wide range of latitude, season, time of day, solar zenith angle, Mars-Sun distance, solar irradiance, and solar wind conditions. We are not concerned with how those parameters vary. We focus here on variations in ionospheric conditions with longitude at fixed latitude. Due to MAVEN’s 5-hr polar orbit, differences in ionospheric conditions at two different longitudes and the same latitude cannot be caused by differences in latitude, season, time of day, solar zenith angle, or Mars-Sun distance. Furthermore, coherent, organized variations in ionospheric conditions with longitude at fixed latitude cannot be caused by temporal variations in solar irradiance or solar wind conditions—unless these temporal variations are periodic with a period commensurate with the MAVEN orbital period, which is unlikely. Hence variations in ionospheric conditions with longitude at fixed latitude must be caused by factors fixed with respect to the solid body of Mars, such as crustal magnetic fields.

In section 3, we use these NGIMS data to examine how ion densities are affected by magnetic field conditions. In section 4, we use these NGIMS data to examine how ionospheric composition is affected by magnetic field conditions.

## 3. Results for Ion Densities

Figures 1a and 1b show how electron density (LPW) and total ion density (NGIMS) at 300–320 km depend on areographic latitude and longitude. Results are similar for the two instruments, which is reassuring. For electron densities and temperatures, Figures 1a and 1c, respectively, can be compared to Figure 1 of Flynn et al. (2017). Despite spanning different time periods, the basic trends in electron density and temperature are similar between this work and Flynn et al. (2017).

Variations with latitude are present in Figures 1a and 1b, but, as discussed by Flynn et al. (2017), can be attributed to temporal changes in periapsis conditions, particularly solar zenith angle and season, over the observing period. Striking variations with longitude at southern latitudes are present in Figures 1a and 1b. MAVEN’s periapsis longitude changes appreciably from one periapsis to the next as Mars rotates beneath MAVEN’s orbital plane, while other factors like periapsis latitude and solar zenith angle change more slowly. As in Flynn et al. (2017), it is clear that the longitudinal structure apparent at southern latitudes in

NASA Author Manuscript NASA Author Manuscript NASA Author Manuscript

Figures 1a and 1b is caused by regions of crustal magnetic fields, which are strongest at southern latitudes and roughly 120°E to 240°E.

Figures 1d–1f show how individual ion densities measured by NGIMS at 300–320 km depend on areographic latitude and longitude. We focus on $O_2^+$, $O^+$, and $CO_2^+$ as the most significant ionospheric species (Benna et al., 2015). $O_2^+$ densities display clear dependence on longitude at southern latitudes and appear to behave similarly to the total ion density. By contrast, $O^+$ and $CO_2^+$ densities have less apparent dependences on longitude. This excludes the simplest possible scenario in which densities of all ion species vary in the same manner as crustal magnetic field conditions change with longitude. Therefore we present a more detailed survey of spatial variations in ion densities and composition. Having established that NGIMS ion densities vary coherently with longitude at southern latitudes, we henceforth use only ion densities south of 30°S, which is consistent with Flynn et al. (2017).

Figure 2 shows various NGIMS ion densities as functions of altitude and longitude. The total ion density panel shows similar behavior to Figure 2a of Flynn et al. (2017). Above 200 km, densities are larger at longitudes where crustal magnetic fields are strong (120°E to 240°E) than at other longitudes. Similar trends are seen in the $O_2^+$ panel. Comparable trends are also seen in the $O^+$ and $CO_2^+$ panels. For $O^+$ and $CO_2^+$, however, variations with longitude are not apparent until higher altitudes.

Figure 3 shows how various NGIMS ion densities vary with altitude in selected longitude bins. In the selected longitude bins and at altitudes of 200 km and above, both total ion density and $O_2^+$ density are noticeably greater in strongly magnetized regions than in weakly magnetized regions. Similarly, in the selected longitude bins and at altitudes of 290 km and above, both $O^+$ density and $CO_2^+$ density are noticeably greater in strongly magnetized regions than in weakly magnetized regions. For practically all ion species measured by NGIMS, the supporting information that accompanies this manuscript shows that densities are greater in strongly magnetized regions than in weakly magnetized regions above some threshold altitude. However, the threshold altitude is species-dependent.

Figure 4a shows how the dependence of ion densities on altitude differs between strongly magnetized regions and weakly magnetized regions. The threshold altitude above which differences are apparent is lower for total ion density and $O_2^+$ density than for $O^+$ density and $CO_2^+$ density. Scale heights are greater in strongly magnetized regions than in weakly magnetized regions.

Figure 4b shows how the ratio of ion density in strongly magnetized regions to ion density in weakly magnetized regions varies with altitude for several ion species. As previously noted, density enhancement in strong field regions relative to weak field regions is apparent at high altitudes for all three individual species and for the total ion density. Moreover, differences in threshold altitude by species are also apparent. For all three individual species, the ratio of densities appears to increase approximately exponentially with altitude. For $CO_2$, this trend

NASA Author Manuscript NASA Author Manuscript NASA Author Manuscript

is visible between approximately 270 and 370 km. At lower altitudes, strong-field and weak-field densities are similar. At higher altitudes, densities are small and hence have large fractional uncertainties. This causes the exponential trend to break down. Furthermore, the scale height associated with that exponential dependence increases from $CO_2^+$ to $O_2^+$ to $O^+$, a trend that is consistent with the common inverse proportionality between scale height and species mass. We suggest that reproduction of these behaviors will be an important metric for tests of any hypotheses that are proposed to explain the observational results reported in this article.

## 4. Results for Ionospheric Composition

Figures 5a–5c show the effects of these changes in ion density on ionospheric composition. In this representation, the fractional abundance of $O_2^+$ appears greater in strongly magnetized regions than in weakly magnetized regions at altitudes above about 280 km. The fractional abundance of $O^+$ appears smaller in strongly magnetized regions than in weakly magnetized regions at altitudes above about 280 km. The fractional abundance of $CO_2^+$ appears smaller in strongly magnetized regions than in weakly magnetized regions at altitudes above about 220 km. Above 200-km altitude, the fractional abundance of $NO^+$ is smaller in strongly magnetized regions than in weakly magnetized regions.

Figures 4c and 5d show how the dependence of ionospheric composition on altitude differs between strongly magnetized regions and weakly magnetized regions. The bulk composition of the ionosphere differs markedly between strongly magnetized and weakly magnetized regions. In strongly magnetized regions, the high-altitude $O^+/O_2^+$ ratio is approximately 0.5 and the plasma composition is predominantly $O_2^+$. In weakly magnetized regions, the high-altitude $O^+/O_2^+$ ratio is approximately 0.8 and the plasma composition is a near-equal mix of $O^+$ and $O_2^+$. Figure 5d confirms that these regions of distinct composition are spatially coherent.

## 5. Consideration of Possible Instrumental Effects

NGIMS ion density measurements are sensitive to the ion flow velocity (Mahaffy et al., 2015). If the ion flow velocity has a strong dependence on magnetic field conditions, then the apparent dependence of the reported ion density measurements on magnetic field conditions could be biased. The agreement shown in Figures 1a and 1b between NGIMS total ion density and LPW electron density, which is not sensitive to ion flow velocity, suggests that this possibility is unlikely. Nevertheless, in order to more firmly exclude this possibility, we also examined ion densities measured by the MAVEN STATIC instrument. STATIC consists of “a toroidal ‘top hat’ electrostatic analyzer [and] a time-of-flight velocity analyzer” (McFadden et al., 2015). Its density measurements are not sensitive to ion flow velocity. Figure 6 shows vertical profiles of STATIC dayside total, $O^+$, and $O_2^+$ densities in strongly and weakly magnetized regions. $CO_2^+$ densities are not shown as reliable values have not been derived from these data. Data are from October 2014 to March 2018 and

NASA Author Manuscript NASA Author Manuscript NASA Author Manuscript

latitudes poleward of 30°S. As the STATIC ion density observations in Figure 6 are consistent with the independent NGIMS ion density observations in Figure 4a, we conclude that both sets of density measurements are reliable.

## 6. Dependence of Neutral Conditions on Magnetic Field Environment

The neutral atmosphere is not as strongly influenced by magnetic field conditions. Figure 7 shows NGIMS densities of neutral Ar, CO, O, $N_2$, and $CO_2$ at 200- to 300-km altitude at solar zenith angles of less than 90° in strongly and weakly magnetized regions. Densities at higher altitudes are not reliable due to low count rates. Data are from February 2015 to March 2018 at latitudes poleward of 30°S. No appreciable neutral density differences are apparent between strongly magnetized regions and weakly magnetized regions. Hence the observed dependence of ion densities and ionospheric composition on magnetic field conditions must be caused by processes that do not require associated variations in neutral atmospheric conditions.

## 7. Conclusions

Densities of ion species in the ionosphere of Mars depend on magnetic field conditions. Above ~200 km, ion densities are tens of percent greater in strongly magnetized regions than in weakly magnetized regions. At lower altitudes, densities are not dependent on the magnetic field environment. This is consistent with earlier work using electron densities (Flynn et al., 2017). This result applies to the individual ion species $O_2^+$, $O^+$, and $CO_2^+$, as shown here, and to many other ion species that are shown in the supporting information that accompanies this manuscript. However, the altitude at which ion densities show appreciable dependence on longitude is species-dependent.

The ionospheric composition is also affected by magnetic field conditions. At high altitudes above 200 km, the fractional abundances of $O^+$ and $CO_2^+$ are smaller in strongly magnetized regions than in weakly magnetized regions, while the fractional abundance of $O_2^+$ is greater in strongly magnetized regions than in weakly magnetized regions. Thus the bulk composition of the high-altitude ionosphere differs markedly between strongly magnetized and weakly magnetized regions. At lower altitudes, the composition is not dependent on the magnetic field environment. In strongly magnetized regions, the $O^+/O_2^+$ ratio is approximately 0.5 and the plasma composition is predominantly $O_2^+$. In weakly magnetized regions, the $O^+/O_2^+$ ratio is approximately 0.8 and the plasma composition is a near-equal mix of $O^+$ and $O_2^+$. Consequently, the plasma reservoir available for escape is fundamentally different between strongly magnetized and weakly magnetized regions.

The physical reasons for these differences require explanation, and we suggest that data-verified numerical simulations be performed to explain these observations. Although a full treatment is beyond the scope of the current work, here we consider possible reasons why crustal magnetic fields affect densities of individual ion species and the composition of the ionosphere.

NASA Author Manuscript NASA Author Manuscript NASA Author Manuscript

As outlined in section 1, theoretical justifications have been set forth for the observed dependence of electron temperature on magnetic field conditions. There are several ways in which these electron temperature variations may affect ion densities and explain the observations reported here. Electron temperature affects chemical loss rates of ions. Dissociative recombination rate coefficients for molecular ions generally decrease as electron temperature increases (Schunk & Nagy, 2009). This directly affects molecular ion densities (e.g., $O_2^+$ and $CO_2^+$). It affects different molecular ion species differently since the temperature dependence of these rate coefficients is not identical for all species. Also, atomic ion densities are indirectly affected. Radiative recombination of atomic ions is generally slow (Schunk & Nagy, 2009), so the dominant loss mechanisms for atomic ions generally involve conversion to a molecular ion via a charge exchange reaction, followed by dissociative recombination at a rate dependent on electron temperature. Electron temperature affects the transport of ions. Temperature affects pressure gradients both directly and indirectly: directly, because pressure is proportional to the product of density and temperature, and indirectly, because density depends on temperature as noted above. Higher temperatures imply higher pressure both directly and indirectly. Higher temperatures suppress chemical loss rates and hence increase densities, which augments the direct proportionality of pressure to temperature. Therefore a given change in electron temperature affects pressure gradients for individual species differently. Changes in transport-controlled density can be seen clearly in the idealized case of diffusive equilibrium. Here the plasma scale height is proportional to the ratio of temperature to ion mass, and thus different ion species are affected differently by a given change in electron temperature.

## Supplementary Material

Refer to Web version on PubMed Central for supplementary material.

## Acknowledgments

MAVEN data are available from the PPI node of the NASA Planetary Data System (https://pds-ppi.igpp.ucla.edu/mission/MAVEN/). The MAVEN project is supported by NASA through the Mars Exploration Program. P. W. and C. F. acknowledge support from the MAVEN project. M. V. acknowledges support from NASA award 80NSSC17K0735. G. L. acknowledges support from NASA award NNX16AJ42G.

## References

Acuña MH, Connerney JEP, Ness NF, Lin RP, Mitchell D, Carlson CW, et al. (1999). Global distribution of crustal magnetization discovered by the Mars Global Surveyor MAG/ER Experiment. Science, 284, 790–793. 10.1126/science.284.5415.790 [PubMed: 10221908]

Acuña MH, Connerney JEP, Wasilewski P, Lin RP, Mitchell D, Anderson KA, et al. (2001). Magnetic field of Mars: Summary of results from the aerobraking and mapping orbits. Journal of Geophysical Research, 106, 23,403–23,418. 10.1029/2000JE001404

Andersson L, Ergun RE, Delory GT, Eriksson A, Westfall J, Reed H, et al. (2015). The Langmuir Probe and Waves (LPW) Instrument for MAVEN. Space Science Reviews, 195, 173–198. 10.1007/s11214-015-0194-3

Andrews DJ, Andersson L, Delory GT, Ergun RE, Eriksson AI, Fowler CM, et al. (2015). Ionospheric plasma density variations observed at Mars by MAVEN/LPW. Geophysical Research Letters, 42, 8862–8869. 10.1002/2015GL065241

NASA Author Manuscript NASA Author Manuscript NASA Author Manuscript

Andrews DJ, Edberg NJT, Eriksson AI, Gurnett DA, Morgan D, Němec F, & Opgenoorth HJ (2015). Control of the topside Martian ionosphere by crustal magnetic fields. Journal of Geophysical Research: Space Physics, 120, 3042–3058. 10.1002/2014JA020703

Benna M, Mahaffy PR, Grebowsky JM, Fox JL, Yelle RV, & Jakosky BM (2015). First measurements of composition and dynamics of the Martian ionosphere by MAVEN's Neutral Gas and Ion Mass Spectrometer. Geophysical Research Letters, 42, 8958–8965. 10.1002/2015GL066146

Brain DA, Bagenal F, Acuña MH, & Connerney JEP (2003). Martian magnetic morphology: Contributions from the solar wind and crust. Journal of Geophysical Research, 108(A12), 1424 10.1029/2002JA009482

Brecht SH, & Ledvina SA (2014). The role of the Martian crustal magnetic fields in controlling ionospheric loss. Geophysical Research Letters, 41, 5340–5346. 10.1002/2014GL060841

Cain JC, Ferguson BB, & Mozzoni D (2003). An $n = 90$ internal potential function of the Martian crustal magnetic field. Journal of Geophysical Research, 108(E2), 5008 10.1029/2000JE001487

Connerney JEP, Acuña MH, Wasilewski PJ, Kletetschka G, Ness NF, Rème H, et al. (2001). The global magnetic field of Mars and implications for crustal evolution. Geophysical Research Letters, 28, 4015–4018. 10.1029/2001GL013619

Connerney JEP, Acuna MH, Wasilewski PJ, Ness NF, Reme H, Mazelle C, et al. (1999). Magnetic lineations in the ancient crust of Mars. Science, 284, 794 10.1126/science.284.5415.794 [PubMed: 10221909]

Dong C, Bougher SW, Ma Y, Toth G, Lee Y, Nagy AF, et al. (2015). Solar wind interaction with the Martian upper atmosphere: Crustal field orientation, solar cycle, and seasonal variations. Journal of Geophysical Research: Space Physics, 120, 7857–7872. 10.1002/2015JA020990

Edberg NJT, Lester M, Cowley SWH, & Eriksson AI (2008). Statistical analysis of the location of the Martian magnetic pileup boundary and bow shock and the influence of crustal magnetic fields. Journal of Geophysical Research, 113, A08206 10.1029/2008JA013096

Ergun RE, Morooka MW, Andersson LA, Fowler CM, Delory GT, Andrews DJ, et al. (2015). Dayside electron temperature and density profiles at Mars: First results from the MAVEN Langmuir Probe and Waves instrument. Geophysical Research Letters, 42, 8846–8853. 10.1002/2015GL065280

Fang X, Ma Y, Masunaga K, Dong Y, Brain D, Halekas J, et al. (2017). The Mars crustal magnetic field control of plasma boundary locations and atmospheric loss: MHD prediction and comparison with MAVEN. Journal of Geophysical Research: Space Physics, 122, 4117–4137. 10.1002/2016JA023509

Flynn CL, Vogt MF, Withers P, Andersson L, England S, & Liu G (2017). MAVEN observations of the effects of crustal magnetic fields on electron density and temperature in the Martian dayside ionosphere. Geophysical Research Letters, 44, 10,812–10,821. 10.1002/2017GL075367

Girazian Z, Mahaffy P, Lillis RJ, Benna M, Elrod M, Fowler CM, & Mitchell DL (2017). Ion densities in the nightside ionosphere of Mars: Effects of electron impact ionization. Geophysical Research Letters, 44, 11,248–11,256. 10.1002/2017GL075431

Mahaffy PR, Benna M, King T, Harpold DN, Arvey R, Barciniak M, et al. (2015). The Neutral Gas and Ion Mass Spectrometer on the Mars Atmosphere and Volatile Evolution mission. Space Science Reviews, 195, 49–73. 10.1007/s11214-014-0091-1

McFadden JP, Kortmann O, Curtis D, Dalton G, Johnson G, Abiad R, et al. (2015). MAVEN SupraThermal and Thermal Ion Compostion (STATIC) instrument. Space Science Reviews, 195, 199–256. 10.1007/s11214-015-0175-6

Mitchell DL, Lin RP, Mazelle C, Rème H, Cloutier PA, Connerney JEP, et al. (2001). Probing Mars' crustal magnetic field and ionosphere with the MGS Electron Reflectometer. Journal of Geophysical Research, 106, 23,419–23,428.

Sakai S, Andersson L, Cravens TE, Mitchell DL, Mazelle C, Rahmati A, et al. (2016). Electron energetics in the Martian dayside ionosphere: Model comparisons with MAVEN data. Journal of Geophysical Research: Space Physics, 121, 7049–7066. 10.1002/2016JA022782

Schunk RW, & Nagy AF (2009). Ionospheres, second edition New York: Cambridge University Press.

NASA Author Manuscript

NASA Author Manuscript

NASA Author Manuscript

**Key Points:**

- Densities of all ion species are enhanced in strong crustal field regions
- Ionospheric composition above 200 km depends on magnetic field conditions
- The $O^+/O_2^+$ ratio is smaller in strong crustal field regions

NASA Author Manuscript NASA Author Manuscript NASA Author Manuscript

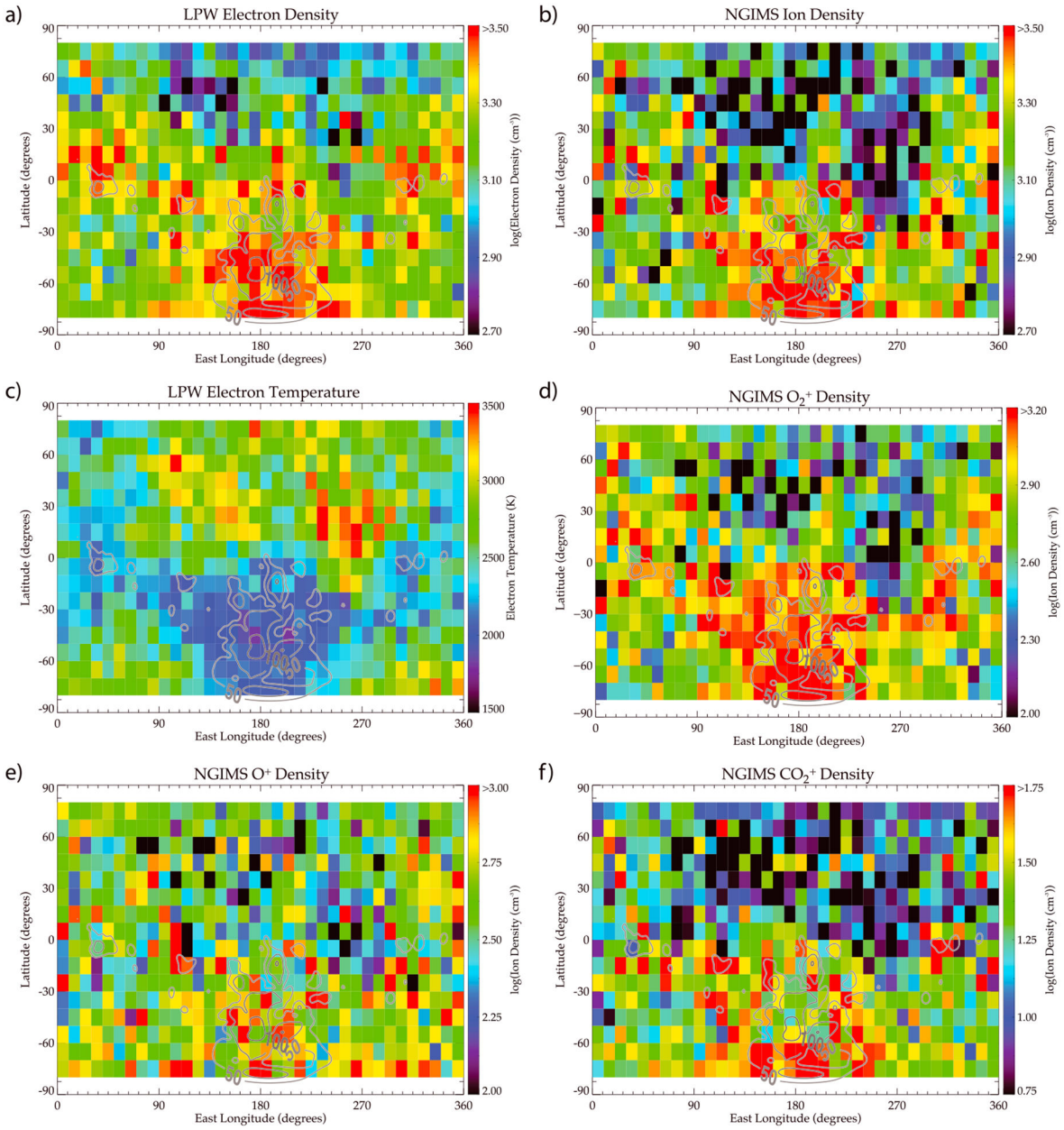


**Figure 1.**

(a) LPW electron density at 300- to 320-km altitude as a function of areographic latitude and longitude. The color indicates the median value in a 10° by 10° latitude-longitude bin. White bins contain fewer than five data points. Gray contours show magnetic field magnitudes (Cain et al., 2003) of 50, 100, and 200 nT at 310 km. (b) As panel (a) but for NGIMS total ion density. (c) As panel (a) but for LPW electron temperature. (d) As panel (a) but for NGIMS $O_2^+$ ion density. (e) As panel (a) but for NGIMS $O^+$ ion density. (f) As panel (a) but for NGIMS $CO_2^+$ ion density. LPW = Langmuir Probe and Waves; NGIMS = Neutral Gas and Ion Mass Spectrometer.

NASA Author Manuscript

NASA Author Manuscript

NASA Author Manuscript

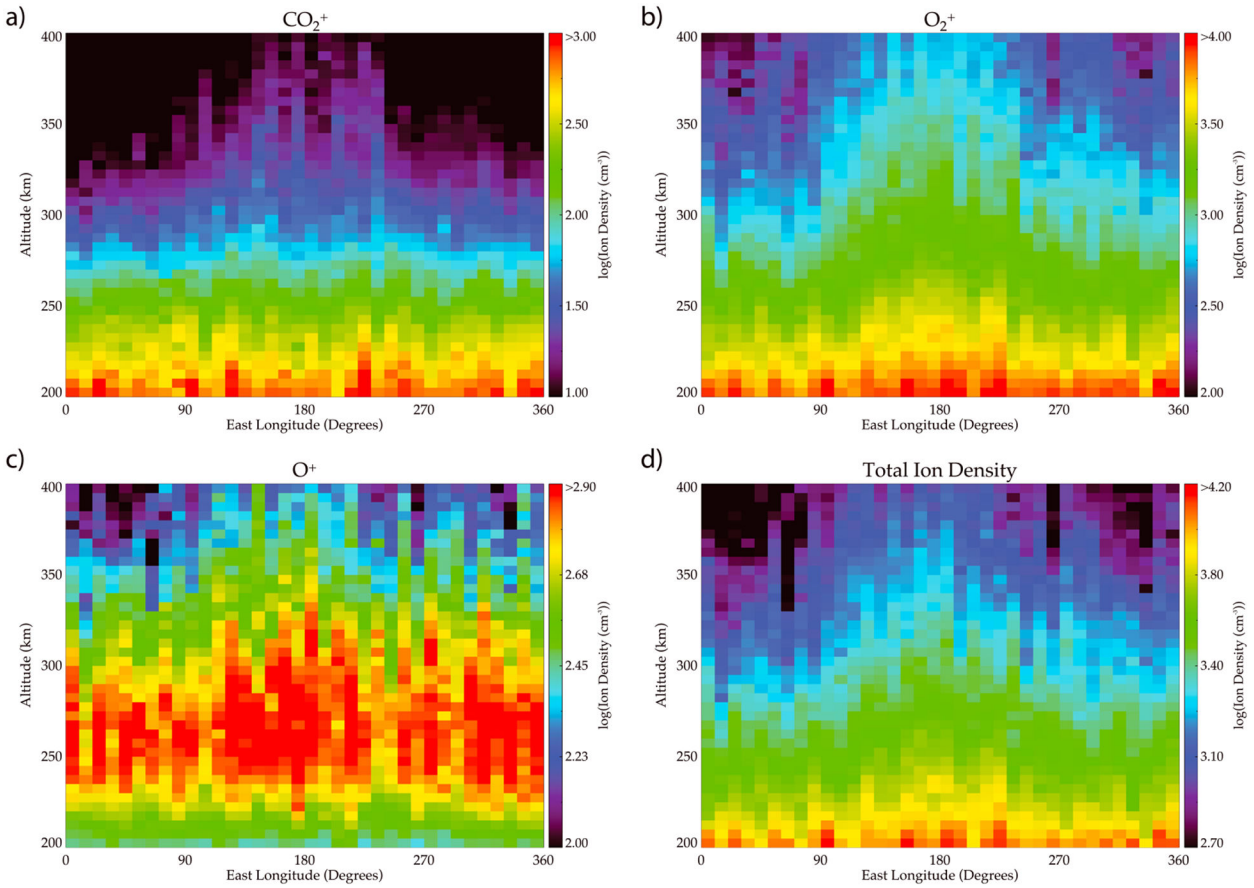


**Figure 2.**

(a) Neutral Gas and Ion Mass Spectrometer (NGIMS) $CO_2^+$ ion density as a function of altitude and areographic longitude from areographic latitudes poleward of 30°S and solar zenith angles less than 90°. The color indicates the median value in each 5-km altitude by 10° longitude bin. White bins contain fewer than five data points.(b) As panel (a) but for NGIMS $O_2^+$ ion density. (c) As panel (a) but for NGIMS $O^+$ ion density. (d) As panel (a) but for NGIMS total ion density.

NASA Author Manuscript NASA Author Manuscript NASA Author Manuscript

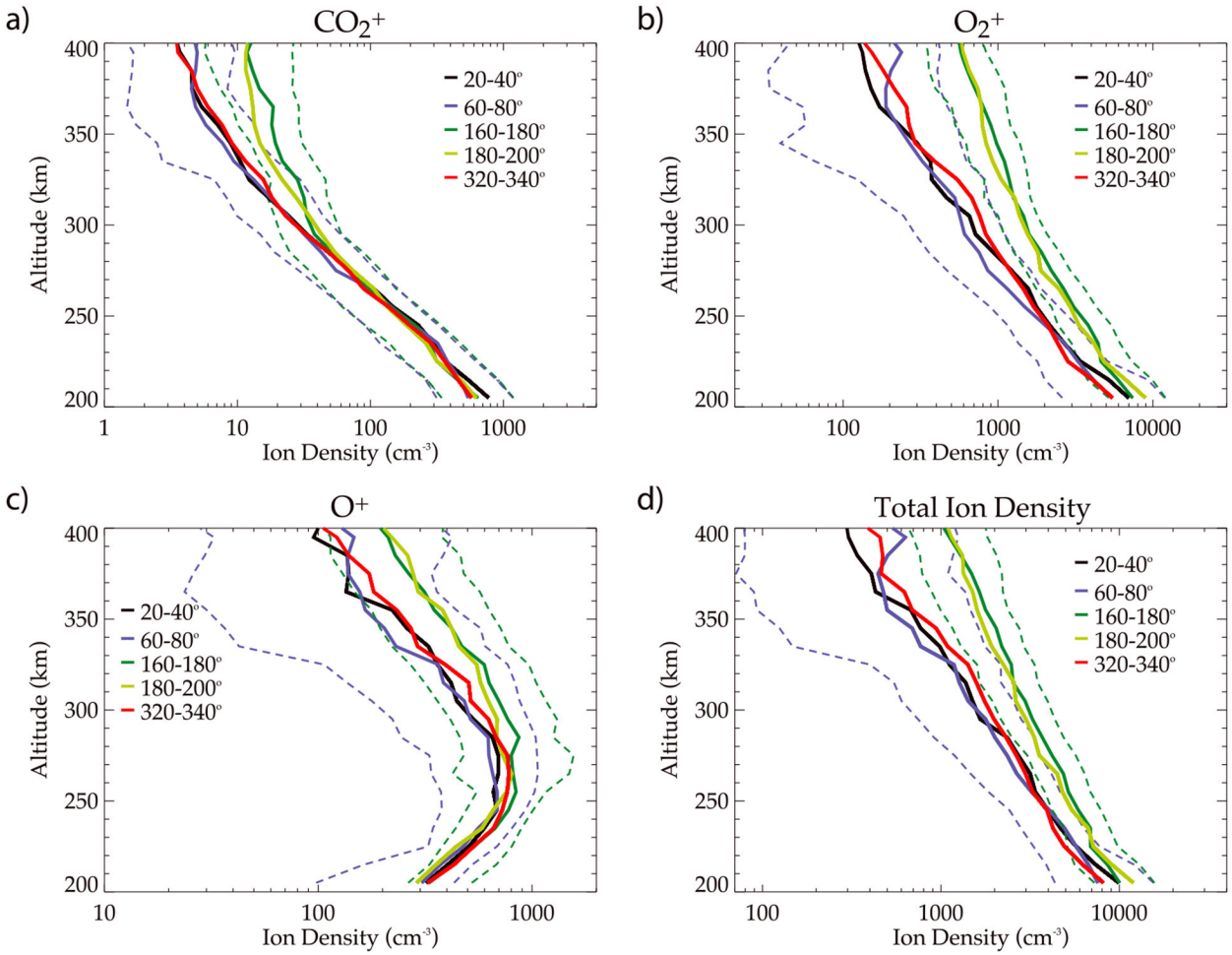


**Figure 3.**

(a) Median Neutral Gas and Ion Mass Spectrometer (NGIMS) $CO_2^+$ ion density altitude profiles, calculated using data from latitudes poleward of 30°S and solar zenith angles less than 90°, and five different longitude ranges: 20–40°E (black), 60–80°E (blue), 160–180°E (dark green), 180–200°E (light green), and 320–340°E (red). The dashed lines show upper and lower quartiles for data at 60–80°E (weak crustal fields) and 160–180°E (strong crustal fields). (b) As panel (a) but for NGIMS $O_2^+$ ion density. (c) As panel (a) but for NGIMS $O^+$ ion density. (d) As panel (a) but for NGIMS total ion density.

NASA Author Manuscript NASA Author Manuscript NASA Author Manuscript

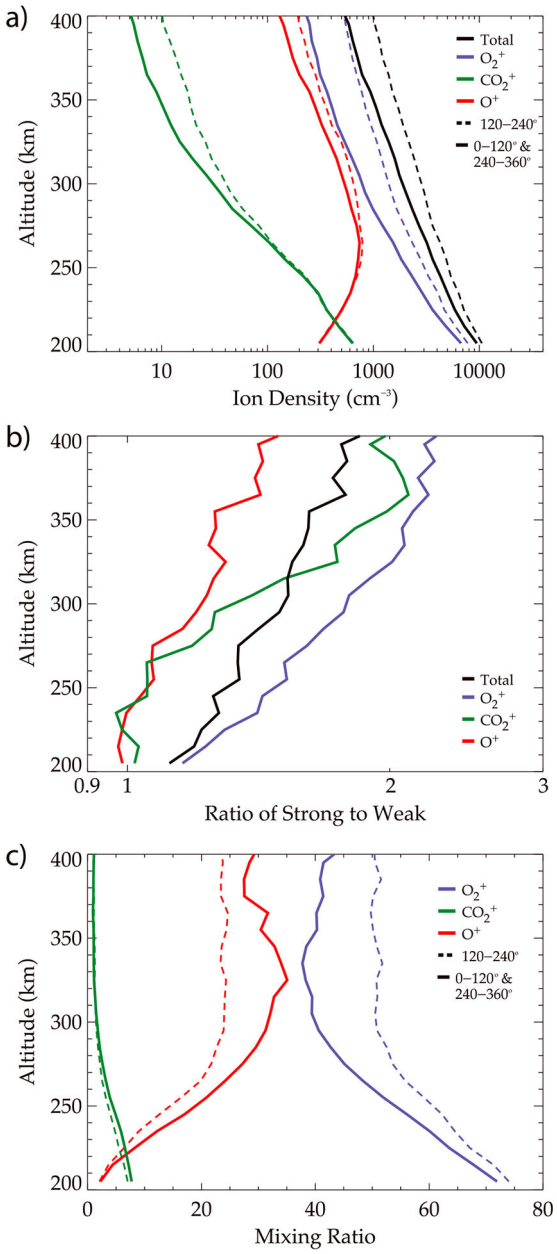


**Figure 4.**

(a) Ion density as a function of altitude in strongly magnetized regions (120–240°E, dashed lines) and weakly magnetized regions (all other longitudes, solid lines). Results are shown for total ions, $O_2^+$, $O^+$, and $CO_2^+$. (b) Ratio of ion density in strong crustal field regions (120–240°E) to ion density in weak crustal field regions (all other longitudes) for various Neutral Gas and Ion Mass Spectrometer ion species as indicated on the figure. (c) Ion mixing ratio (percent) as a function of altitude in strongly magnetized regions (120–240°E, dashed lines) and weakly magnetized regions (all other longitudes, solid lines). Results are shown for $O_2^+$, $O^+$, and $CO_2^+$.

NASA Author Manuscript

NASA Author Manuscript

NASA Author Manuscript

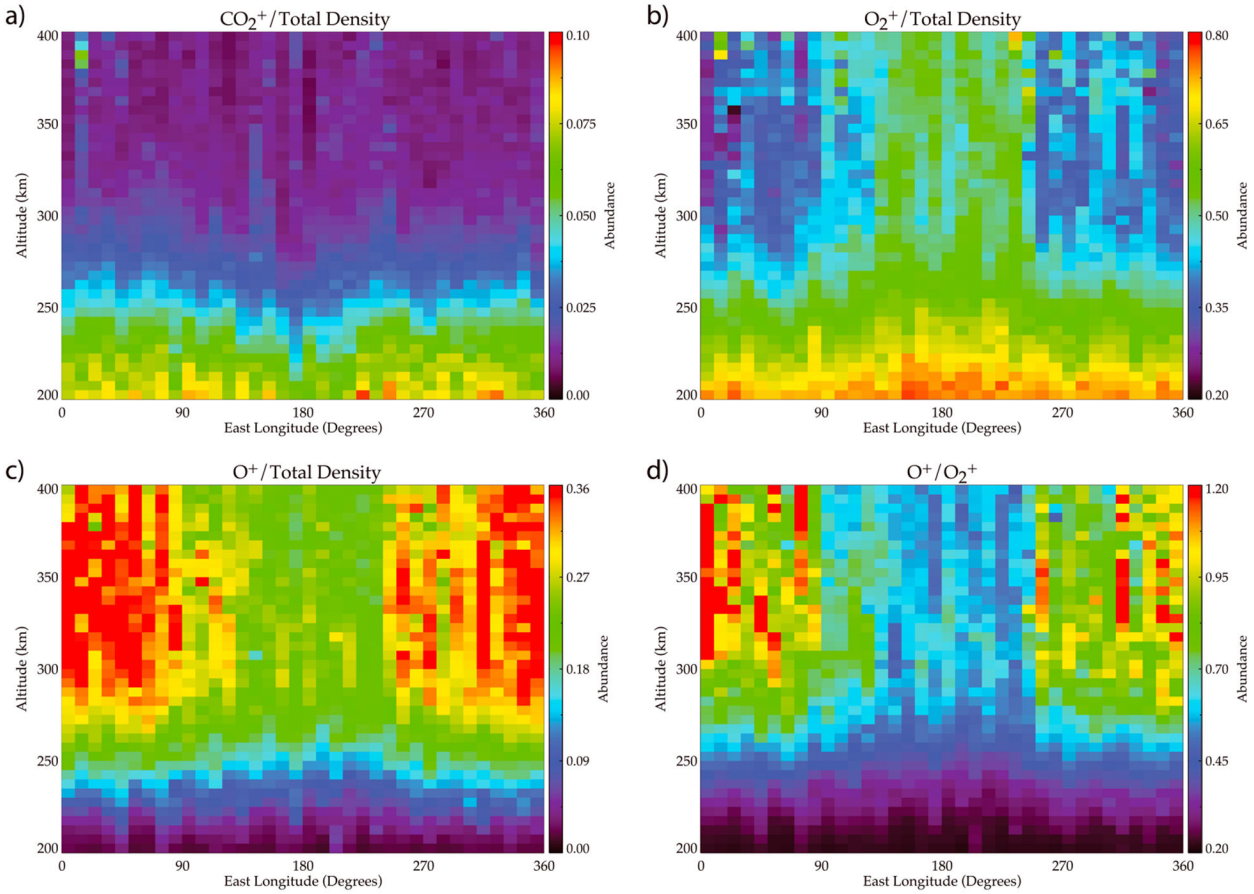


**Figure 5.**

(a) Ratio of $CO_2^+$ density to total ion density as function of altitude and areographic longitude. (b) As panel (a) but for $O_2^+$. (c) As panel (a) but for $O^+$. (d) Ratio of $O^+$ ion density to $O_2^+$ ion density as function of altitude and areographic longitude.

NASA Author Manuscript

NASA Author Manuscript

NASA Author Manuscript

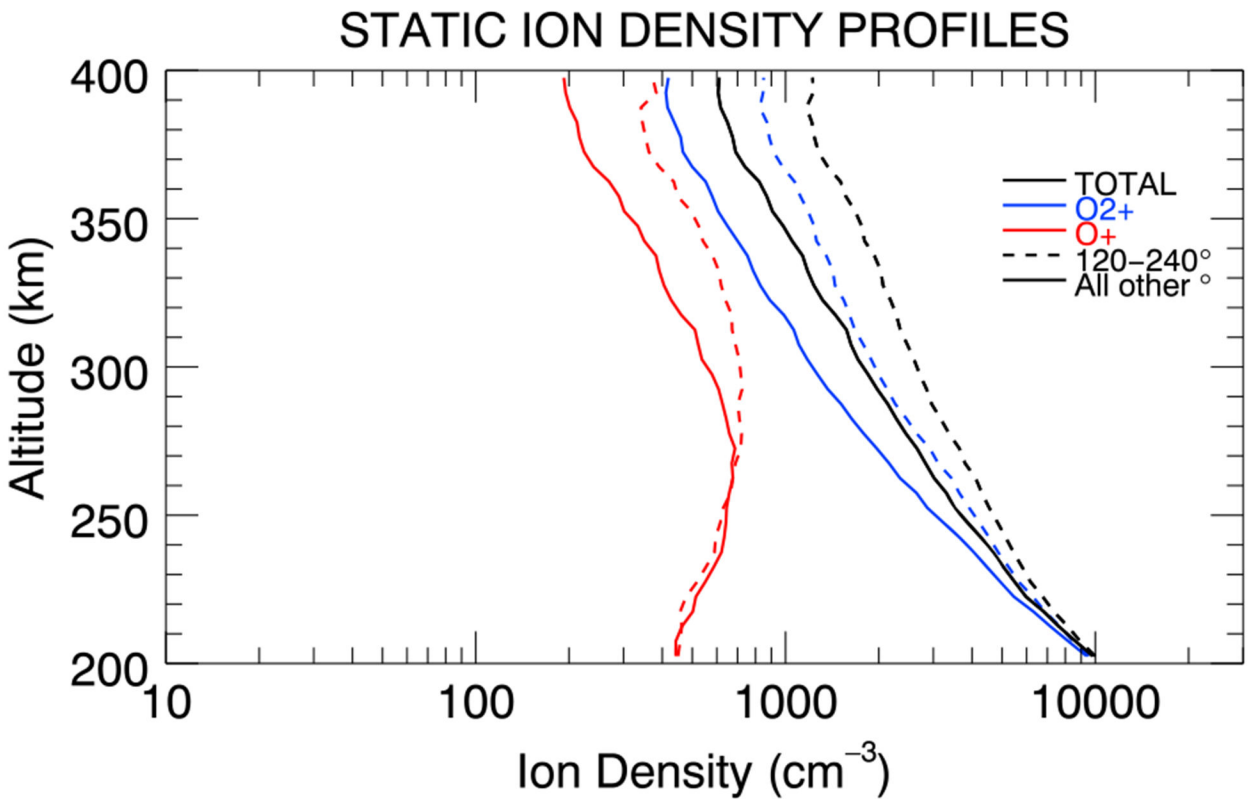


**Figure 6.**
As Figure 4a but using SupraThermal and Thermal Ion Composition (STATIC) data.

NASA Author Manuscript

NASA Author Manuscript

NASA Author Manuscript

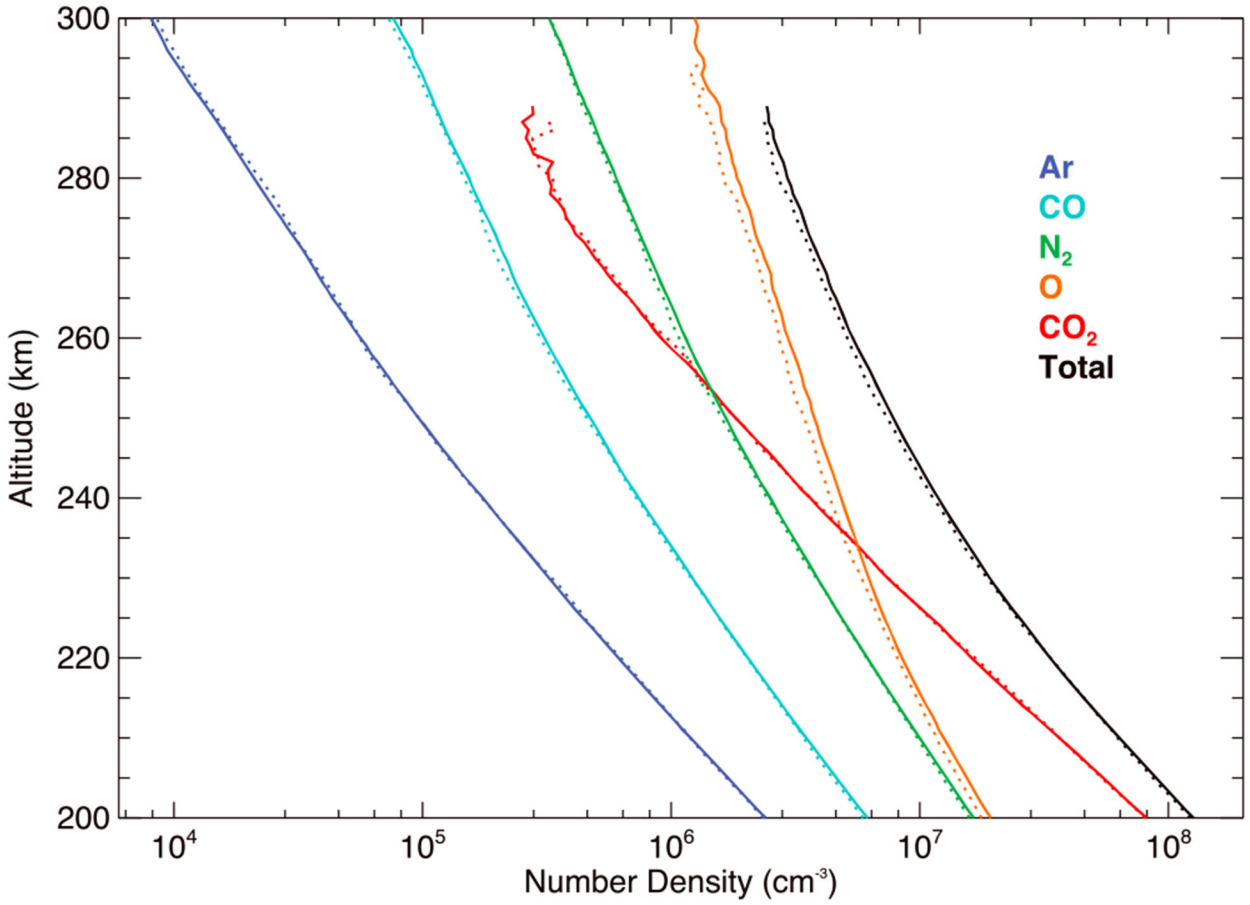


**Figure 7.**

Neutral number density as function of altitude in strongly magnetized regions (120–240°E, dashed lines) and weakly magnetized regions (all other longitudes, solid lines). Results are shown for Ar, CO, $N_2$, O, $CO_2$, and total density.